Journal of the Korean Physical Society, Vol. 52, No. 6, June 2008, pp. 1913∼1917

Stochastic Oscillator Death in Globally Coupled Neural Systems

Woochang LIM* and Sang-Yoon KIM†
Department of Physics, Kangwon National University, Chunchon 200-701

(Received 26 December 2007, in final form 11 March 2008)

We consider an ensemble of globally coupled subthreshold Morris-Lecar neurons. As the coupling strength passes a lower threshold, the coupling stimulates coherence between noise-induced spikings. This coherent transition is well described in terms of an order parameter. However, for sufficiently large J, "stochastic oscillator death" (*i.e.*, quenching of noise-induced spikings), leading to breakup of collective spiking coherence, is found to occur. Using the techniques of nonlinear dynamics, we investigate the dynamical origin of stochastic oscillator death. Thus, we show that stochastic oscillator death occurs because each local neuron is attracted to a noisy equilibrium state via an infinite-period bifurcation. Furthermore, we introduce a new "statistical-mechanical" parameter, called the average firing probability $\overline{P_f}$ and quantitatively characterize a transition from firing to non-firing states which results from stochastic oscillator death. For a firing (non-firing) state, $\overline{P_f}$ tends to be non-zero (zero) in the thermodynamic limit. We note that the role of $\overline{P_f}$ for the firing-nonfiring transition is similar to that of the order parameter used for the coherence-incoherence transition.

PACS numbers: 87.19.La, 05.40.Ca
Keywords: Coupled neural systems, Stochastic oscillator death

I. INTRODUCTION

In recent years, there has been great interest in brain rhythms [1]. Synchronous oscillations in neural systems are correlated with neural encoding of sensory stimuli [2]. Population dynamics has been intensively investigated in coupled systems consisting of spontaneously firing neurons; thus, three types of mechanisms for neural synchronization have been found [3]. Here, we are interested in collective dynamics in neural networks composed of subthreshold neurons. For an isolated single case, each subthreshold neuron cannot fire spontaneously without noise; it can fire only with the help of noise.

In this paper, we consider a large population of globally coupled subthreshold Morris-Lecar (ML) neurons [4–7]. When the coupling strength J is small, the collective state is incoherent because neurons fire independently. However, as J passes a lower threshold J_l^*, a transition to collective spiking coherence occurs because the coupling stimulates coherence between noise-induced spikings. As in globally coupled chaotic systems [8–10], this coherent transition may be described in terms of an order parameter $\mathcal{O}$. However, for sufficiently large J, breakup of collective spiking coherence occurs due to the effect of "stochastic oscillator death" (*i.e.*, quenching of noise-induced spikings). This stochastic oscillator death is in contrast to the deterministic oscillator death occurring in the absence of noise [11–15]. Using the techniques of nonlinear dynamics, we study the dynamical origin of stochastic oscillator death. For large J, the motion of a local state on a noisy limit cycle is strongly non-uniform because the local state spends much time near a point. As J is further increased, such non-uniformity of the motion along the noisy limit cycle is intensified; hence, the average interspike interval increases without bound. Eventually, when passing a threshold J_o^*, such a non-uniform noisy limit cycle transforms to a noisy equilibrium point via an infinite-period bifurcation [16]. Hence, stochastic oscillator death (*i.e.*, cessation of noise-induced spikings) occurs because each local neuron is attracted to a noisy equilibrium state. This stochastic oscillator death leads to a transition from firing to non-firing states. We also introduce a new "statistical-mechanical" parameter, called the average firing probability $\overline{P_f}$ and characterize the firing-nonfiring transition in terms of $\overline{P_f}$. For a firing (non-firing) state, $\overline{P_f}$ tends to be non-zero (zero) in the thermodynamic limit. We note that the role of $\overline{P_f}$ is similar to that of the order parameter $\mathcal{O}$ used for the coherence-incoherence transition.

This paper is organized as follows. In Sec. II, we make both a dynamical analysis for the occurrence of stochastic oscillator death and a characterization of the firing-nonfiring transition in terms of $\overline{P_f}$. Finally, a summary is given in Sec. III.

*E-mail: wclim@kangwon.ac.kr;
†Corresponding Author: sykim@kangwon.ac.kr

II. STOCHASTIC OSCILLATOR DEATH IN GLOBALLY COUPLED ML NEURONS

We consider a system of N globally coupled neurons. As an element in our coupled system, we choose the conductance-based ML neuron model originally proposed to describe the time-evolution pattern of the membrane potential for the giant muscle fibers of barnacles [4–6]. The population dynamics in this neural network is governed by the following set of differential equations:

$$C\frac{dv_i}{dt} = -I_{ion,i} + I_{DC} + D\xi_i + I_{syn,i}, \tag{1a}$$

$$\frac{dw_i}{dt} = \phi\frac{(w_\infty(v_i) - w_i)}{\tau_R(v_i)}, \quad i = 1, \cdots, N, \tag{1b}$$

where

$$I_{ion,i} = I_{Ca,i} + I_{K,i} + I_{L,i} \tag{2a}$$

$$= g_{Ca} m_\infty(v_i)(v_i - E_{Ca}) \tag{2b}$$

$$+ g_K w_i (v_i - E_K) + g_L (v_i - E_L), \tag{2c}$$

$$I_{syn,i} = \frac{J}{N-1}\sum_{j(\neq i)}^{N} \Theta(v_j - v^*), \tag{2d}$$

$$m_\infty(v) = 0.5\left[1 + \tanh\left\{(v - V_1)/V_2\right\}\right], \tag{2e}$$

$$w_\infty(v) = 0.5\left[1 + \tanh\left\{(v - V_3)/V_4\right\}\right], \tag{2f}$$

$$\tau_R(v) = 1/\cosh\left\{(v - V_3)/(2V_4)\right\}. \tag{2g}$$

Here, the state of the ith neuron at a time t (measured in units of ms) is characterized by two state variables: the membrane potential v_i (measured in units of mV) and the slow recovery variable w_i representing the activation of the K^+ current (*i.e.*, the fraction of open K^+ channels). In Eq. (1a), C represents the capacitance of the membrane of each neuron and the time evolution of v_i is governed by four kinds of source currents.

The total ionic current $I_{ion,i}$ of the ith neuron consists of the calcium current $I_{Ca,i}$, the potassium current $I_{K,i}$ and the leakage current $I_{L,i}$. Each ionic current obeys Ohm's law. The constants g_{Ca}, g_K and g_L are the maximum conductances for the ion and the leakage channels and the constants E_{Ca}, E_K and E_L are the reversal potentials at which each current is balanced by the ionic concentration difference across the membrane. Since the calcium current $I_{Ca,i}$ changes much faster than the potassium current $I_{K,i}$, the gate variable m_i for the Ca^{2+} channel is assumed to always take its saturation value $m_\infty(v_i)$. On the other hand, the activation variable w_i for the K^+ channel approaches its saturation value $w_\infty(v_i)$ with a relaxation time $\tau_R(v_i)/\phi$, where τ_R has a dimension of ms and ϕ is a (dimensionless) temperature-like time scale factor.

Each ML neuron is also stimulated by the common DC current I_{DC} and an independent Gaussian white noise ξ [see the second and third terms in Eq. (1a)] satisfying $\langle\xi_i(t)\rangle = 0$ and $\langle\xi_i(t)\ \xi_j(t')\rangle = \delta_{ij}\ \delta(t - t')$, where $\langle\cdots\rangle$ denotes the ensemble average. The noise ξ_i randomly perturbs the strength of the applied current I_{DC} and its intensity is controlled by the parameter D. The last term in Eq. (1a) represents the coupling of the network. Each neuron is connected to all the other ones through global instantaneous pulse-type synaptic couplings. $I_{syn,i}$ of Eq. (2c) represents such a synaptic current injected into the ith neuron. The coupling strength is controlled by the parameter J, $\Theta(x)$ is the Heaviside step function (*i.e.*, $\Theta(x) = 1$ for $x \geq 0$ and $\Theta(x) = 0$ for $x < 0$) and v^* is the threshold value for the spiking state (*i.e.*, for $v_i > v^*$, a local spiking state of the ith neuron appears). Here, we consider the excitatory coupling of $J > 0$ and set $v^* = 0$ mV.

The ML neuron may exhibit either type-I or type-II excitability, depending on the system parameters. Throughout this paper, we consider the case of type-II excitability where $g_{Ca} = 4.4$ mS/cm^2, $g_K = 8$ mS/cm^2, $g_L = 2$ mS/cm^2, $E_{Ca} = 120$ mV, $E_K = -84$ mV, $E_L = -60$ mV, $C = 5\ \mu$F/cm^2, $\phi = 0.04$, $V_1 = -1.2$ mV, $V_2 = 18$ mV, $V_3 = 2$ mV, and $V_4 = 30$ mV [17]. As I_{DC} passes a threshold in the absence of noise, each single type-II ML neuron begins to fire with a nonzero frequency that is relatively insensitive to changes in I_{DC} [18,19]. Numerical integration of Eq. (1) is done using the Heun method [20] (with the time step $\Delta t = 0.01$ ms), which is similar to the second-order Runge-Kutta method and data for (v_i, w_i) $(i = 1, \ldots, N)$ are obtained with the sampling time interval $\Delta t = 1$ ms. For each realization of the stochastic process in Eq. (1), we choose a random initial point $[v_i(0), w_i(0)]$ for the ith $(i = 1, \ldots, N)$ neuron with uniform probability in the range of $v_i(0) \in (-60, 60)$ and $w_i(0) \in (0.1, 0.5)$.

We consider a large population of globally coupled ML neurons for a subthreshold case of $I_{DC} = 84\ \mu$A/cm^2. For an isolated single case, each subthreshold neuron cannot fire spontaneously in the absence of noise and it may generate firings only with the aid of noise. We set $D = 0.3\ \mu\text{A}\cdot\text{ms}^{1/2}/\text{cm}^2$ and numerically study collective coherence of noise-induced spikings by varying the coupling strength J for $N = 10^3$. Emergence of global spiking coherence in the population may be described by the global potential V_G (*i.e.*, the population-averaged membrane potential) and the global recovery variable W_G,

$$V_G(t) = \frac{1}{N}\sum_{i=1}^{N} v_i(t) \quad \text{and} \quad W_G(t) = \frac{1}{N}\sum_{i=1}^{N} w_i(t). \tag{3}$$

For small J, neurons fire independently and hence incoherent states appear. For an incoherent state of $J = 4$ μA/cm^2, the phase portrait of the global state (V_G, W_G) and the time series of the global potential V_G are shown in Figures 1(a) and 1(b), respectively. The global state lies at a noisy equilibrium point and the global potential is nearly stationary. However, as J passes a lower threshold J_l^* ($\simeq 6.7\ \mu$A/cm^2), a coherent transition occurs because the coupling stimulates collective coherence between noise-induced spikings. Then, collective spiking coherence occurs, as shown in Figures 1(c) and 1(d) for

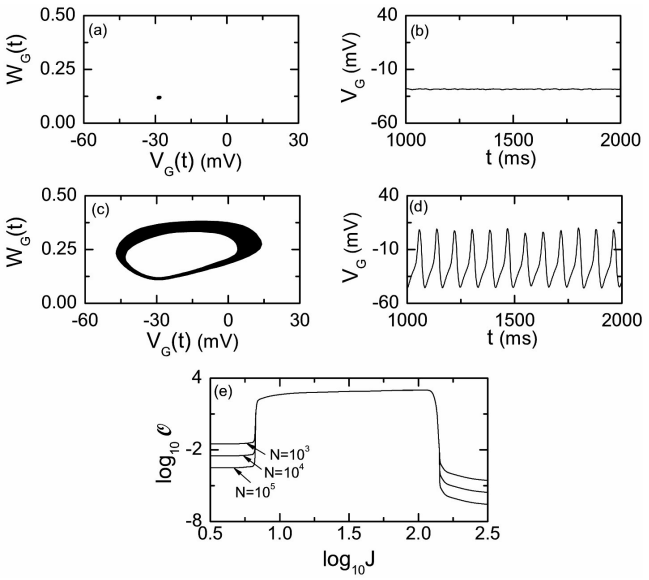

Fig. 1. Coherent and incoherent states for $N = 10^3$ and $D = 0.3\ \mu\text{A} \cdot \text{ms}^{1/2}/\text{cm}^2$. Phase portraits of the global state and the time series of the global potential V_G for $J = 4$ $\mu\text{A}/\text{cm}^2$ [(a) and (b)] and $J = 8$ $\mu\text{A}/\text{cm}^2$ [(c) and (d)]. (e) Plots of $\log_{10}\mathcal{O}$ versus $\log_{10} J$.

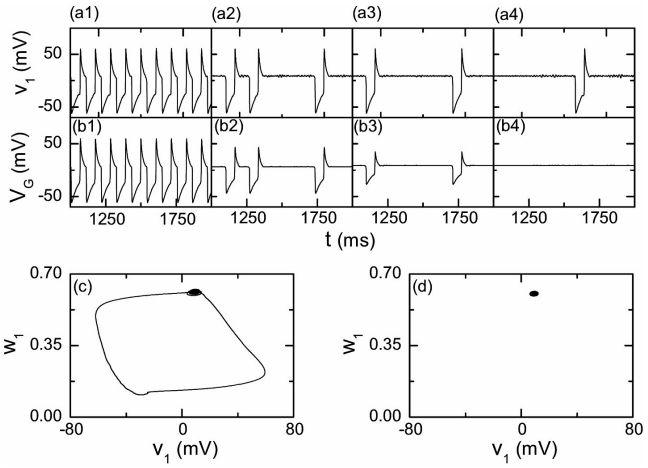

Fig. 2. Dynamical origin for the occurrence of the stochastic oscillator death for $N = 10^3$ and $D = 0.3\ \mu\text{A} \cdot \text{ms}^{1/2}/\text{cm}^2$. Time series of the local potential of the first neuron $v_1(t)$ and the global potential $V_G(t)$ for $J = 141$ [(a1) and (b1)], 141.7 [(a2) and (b2)], 141.8 [(a3) and (b3)] and 142 $\mu\text{A}/\text{cm}^2$ [(a4) and (b4)]. Projections of the noisy equilibrium state onto the $v_1 - w_1$ plane for (c) $J = 142$ and (d) $J = 143$ $\mu\text{A}/\text{cm}^2$.

$J = 8$ $\mu\text{A}/\text{cm}^2$. For this coherent case, the global state exhibits a counterclockwise rotation on a noisy limit cycle; hence, a collective coherent oscillatory motion of the global potential V_G occurs. As in globally coupled chaotic systems [8–10], the mean square deviation of the global potential V_G (*i.e.*, time-averaged fluctuations of V_G),

$$\mathcal{O} \equiv \overline{(V_G(t) - \overline{V_G(t)})^2}, \tag{4}$$

plays the role of the order parameter used for describing the coherence-incoherence transition, where the overbar represents the time averaging. Here, we discard the first time steps of a stochastic trajectory as transients during 10^3 ms; then, we numerically compute $\mathcal{O}$ by following the stochastic trajectory during 10^4 ms. For the coherent (incoherent) state, the order parameter $\mathcal{O}$ approaches a non-zero (zero) limit value in the thermodynamic limit of $N \to \infty$. Figure 1(e) shows a plot of the order parameter versus the coupling strength J. For $J < J_l^*$, incoherent states exist because the order parameter $\mathcal{O}$ tends to zero as $N \to \infty$. As J passes the lower threshold J_l^*, a coherent transition occurs because the coupling stimulates coherence between noise-induced spikings. However, when J passes a higher threshold J_h^* ($\simeq 141.9$ $\mu\text{A}/\text{cm}^2$), such coherent states disappear (*i.e.*, a transition to an incoherent state occurs) due to the effect of stochastic oscillator death occurring for large J (which will be discussed below).

Using the techniques of nonlinear dynamics, we investigate the dynamical origin of stochastic oscillator death, leading to a breakup of collective spiking coherence, for $N = 10^3$. Since our neural network is globally coupled, any local neuron may be a representative one. Figures 2(a1)-2(a4) and 2(b1)-2(b4) show the time series of the local potential $v_1(t)$ of the first neuron and the global potential $V_G(t)$ for $J = 141$, 141.7, 141.8 and 142 $\mu\text{A}/\text{cm}^2$, respectively. The first three cases correspond to coherent (firing) states (with oscillating V_G). With increase in J, the time spent near $v_1(V_G) \simeq 9.3$ mV increases (*i.e.*, the average interspike interval increases) and the amplitude of the global potential V_G decreases. Eventually, when passing the higher threshold J_h^*, a transition to an incoherent (firing) state occurs [*e.g.*, see Figures 2(a4) and 2(b4) for $J = 142$ $\mu\text{A}/\text{cm}^2$, where V_G is nearly stationary because neurons fire independently]. For this incoherent case, the phase portrait of the first local state (v_1, w_1) is shown in Figure 2(c). We note that the motion on the noisy limit cycle is strongly non-uniform because the local state (v_1, w_1) spends much time near the point of $(v_1, w_1) \simeq (9.3, 0.6)$ [*i.e.*, the point density near $(v_1, w_1) \simeq (9.3, 0.6)$ is very high]. As J is increased, such non-uniformity of the motion along the noisy limit cycle is intensified; hence, the average interspike interval increases. Eventually, when passing a threshold J_o^* ($\simeq 142.6$ $\mu\text{A}/\text{cm}^2$), the noisy limit cycle is transformed into a noisy equilibrium point (*e.g.*, see Figure 2(d) for $J = 143$ $\mu\text{A}/\text{cm}^2$), which is similar to the case of an infinite-period bifurcation (also called the saddle-node bifurcation on an invariant circle) in the deterministic case (without noise) [16]. Consequently, stochastic oscillator death (*i.e.*, quenching of noise-induced spikings) occurs for $J > J_o^*$ because each local neuron is attracted to the noisy equilibrium state.

As a result of the stochastic oscillator death, a transi-

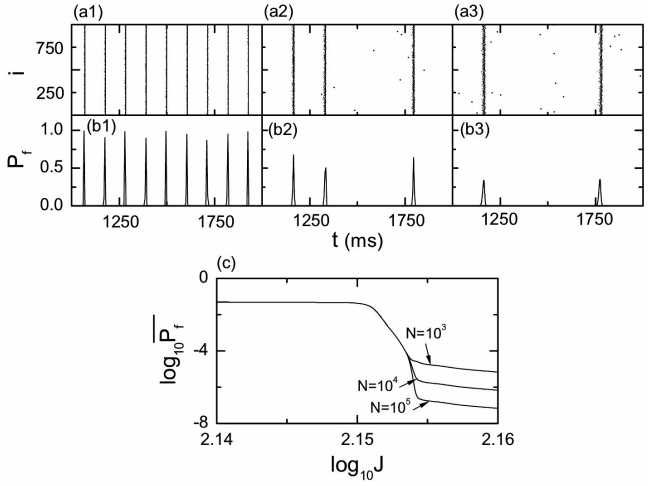

Fig. 3. Characterization of the firing-nonfiring transition for $D = 0.3\ \mu\mathrm{A}\cdot\mathrm{ms}^{1/2}/\mathrm{cm}^2$. Raster plots of neural spikings and firing probabilities P_f for $N = 10^3$ and $J = 141$ [(a1) and (b1)], 141.7 [(a2) and (b2)] and 141.8 $\mu\mathrm{A}/\mathrm{cm}^2$ [(a3) and (b3)]. (c) Plot of $\log_{10}\overline{P_f}$ versus $\log_{10} J$.

tion from firing to non-firing states occurs when passing the threshold J_o^*. We introduce a "statistical-mechanical" parameter, called the average firing probability $\overline{P_f}$ and quantitatively characterize the firing-nonfiring transition in terms of $\overline{P_f}$. Figures 3(a1)-3(a3) show the raster plots of neural spikings (*i.e.*, spatiotemporal plot of neural spikings) for $N = 10^3$ and $J = 141$, 141.7 and 141.8 $\mu\mathrm{A}/\mathrm{cm}^2$, respectively. The raster plot consists of the coherent component (composed of nearly synchronized spikes in the stripes) and the incoherent component (composed of randomly scattered spikes). From each raster plot, one can obtain a firing probability as follows. We divide a long-time interval into bins of width δ (=5 ms) and calculate the firing probability in each bin (*i.e.*, the fraction of firing neurons in each bin),

$$P_f(i) = \frac{N_f(i)}{N}, \tag{5}$$

where $N_f(i)$ is the number of firing neurons in the ith bin ($i = 1, 2, \ldots$) and N is the total number of neurons. For $N = 10^3$, Figures 3(b1)-3(b3) show oscillatory behaviors of P_f for J=141, 141.7 and 141.8 $\mu\mathrm{A}/\mathrm{cm}^2$, respectively. As J is increased, the average oscillating period of P_f increases and the average amplitude of P_f decreases. Thus, a transition to a non-firing state occurs when J exceeds a threshold J_o^* ($\simeq 142.6\mu\mathrm{A}/\mathrm{cm}^2$). For describing this non-firing transition, we introduce the time-average $\overline{P_f}$ of the firing probability over sufficiently many bins,

$$\overline{P_f} = \frac{1}{N_b}\sum_{i=1}^{N_b} P_f(i), \tag{6}$$

where N_b is the number of bins for averaging. For numerical calculation of $\overline{P_f}$, the first time steps during 10^3 ms are discarded as transients; then, the averaging is performed over sufficiently large number of bins ($N_b = 4000$). We note that the role of the average firing probability $\overline{P_f}$ is similar to that of the order parameter $\mathcal{O}$ (used for the coherence-incoherence transition). For the firing (nonfiring) state, the average firing probability $\overline{P_f}$ approaches a nonzero (zero) limit value in the thermodynamic limit of $N \to \infty$. Figure 3(c) shows a plot of the average firing probability $\overline{P_f}$ versus the coupling strength. We note that for $J > J_o^*$, non-firing states appear because $\overline{P_f}$ tends to zero in the thermodynamic limit.

III. SUMMARY

We have numerically studied stochastic oscillator death by varying the coupling strength J in a population of globally coupled subthreshold ML neurons. For sufficiently large J, breakup of collective spiking coherence occurs due to the effect of stochastic oscillator death. Using the techniques of nonlinear dynamics (*e.g.*, time series of the membrane potentials and the local phase portraits), we investigated dynamical origin of the stochastic oscillator death. Thus, we showed that stochastic oscillator death occurs because each local neuron is attracted to a noisy equilibrium point via an infinite-period bifurcation. This stochastic oscillator death leads to a transition from firing to non-firing states. To quantitatively characterize the firing-nonfiring transition, we have introduced a new statistical-mechanical parameter, called the average firing probability $\overline{P_f}$. (The role of $\overline{P_f}$ is similar to that of the order parameter $\mathcal{O}$ used for the coherence-incoherence transition.) For a firing (non-firing) state, $\overline{P_f}$ goes to non-zero (zero) in the thermodynamic limit. Finally, in connection with oscillator death of the single ML neuron, we make some qualitative comments on why stochastic oscillator death occurs for large J. For the single ML neuron, oscillator death occurs through stabilization of an unstable equilibrium point for sufficiently large value of the DC current I_{DC} [5]. That is, when the strength of a stimulus is large, quenching of neural spikings occurs. For our coupled case, in addition to I_{DC}, the synaptic current also stimulates each local neuron. The value of I_{DC} is not large for our subthreshold case. However, for large J, where collective spiking coherence occurs, the magnitude of the synaptic current becomes large. Hence, the strength of the total stimulus (given to each local neuron) becomes large, which might lead to the oscillator death, as in the single case.

ACKNOWLEDGMENTS

This work was supported by the Korea Research Foundation funded by the Korean Government (MOEHRD) (KRF-2006-521-C00062).

REFERENCES

[1] G. Buzsáki, *Rhythms of the Brain* (Oxford University Press, New York, 2006).
[2] C. M. Gray, J. Compu. Neurosci. **1**, 11 (1994).
[3] X.-J. Wang, in *Encyclopedia of Cognitive Science*, edited by L. Nadel (MacMillan, London, 2003), p. 272.
[4] C. Morris and H. Lecar, Biophys. J. **35**, 193 (1981).
[5] J. Rinzel and B. Ermentrout, in *Methods in Neural Modeling: from Ions to Networks*, edited by C. Koch and I. Segev (MIT Press, Cambridge, 1998), p. 251.
[6] K. Tsumoto, H. Kitajima, T. Yoshinaga, K. Aihara and H. Kawakami, Neurocomputing **69**, 293 (2006).
[7] W. Lim and S.-Y. Kim, J. Korean Phys. Soc. **51**, 1427 (2007).
[8] S.-J. Baek and E. Ott, Phys. Rev. E **69**, 066210 (2004).
[9] D. Topaj, W.-H. Kye and A. Pikovsky, Phys. Rev. Lett. **87**, 074101 (2001); A. S. Pikovsky, M. G. Rosenblum and J. Kurths, Europhys. Lett. **34**, 165 (1996).
[10] H. Sakaguchi, Phys. Rev. E **61**, 7212 (2000).
[11] K. Bar-Eli, Physica D **14**, 242 (1985).
[12] D. G. Aranson, G. B. Ermentrout and N. Kopell, Physica D **41**, 403 (1990).
[13] G. B. Ermentrout and N. Kopell, SIAM J. Appl. Math. **50**, 125 (1990).
[14] Z. Neufeld, I. Z. Kiss, C. Zhou and J. Kurths, Phys. Rev. Lett. **91**, 084101 (2003).
[15] S. D. Monte, F. d'Ovidio and E. Mosekilde, Phys. Rev. Lett. **90**, 054102 (2003).
[16] S. H. Strogatz, *Nonlinear Dynamics and Chaos: With Applications to Physics, Biology, Chemistry and Engineering* (Addition-Wesley, Reading, MA, 1994), p. 262.
[17] The values of the parameters are the same as those in Ref. [5] except for the membrane capacitance C; more coherent states seem to appear for smaller C.
[18] A. L. Hodgkin, J. Physiol. **107**, 165 (1948).
[19] E. M. Izhikevich, Int. J. Bifurcation Chaos **10**, 1171 (2000).
[20] M. San Miguel and R. Toral, in *Instabilities and Nonequilibrium Structures VI*, edited by J. Martinez, R. Tiemann and E. Tirapegui (Kluwer Academic Publisher, Dordrecht, 2000), p. 35.